Drug Design, Development and Therapy

Dovepress
open access to scientific and medical research

Open Access Full Text Article

ORIGINAL RESEARCH

Fenofibrate Ameliorates Retinal Pigment Epithelium Injury Induced by Excessive Fat Through Upregulation of PI3K/AKT Signaling

Xue Wang[1–3], Xiaomei Liu[2], Radouil Tzekov[4], Chaofeng Yu[1], Jiasong Yang[1,5], Yuliang Feng[1], Yajun Wu[1], Yali Xu[1], Shiying Li[6], Wensheng Li[1,5,7]

[1]Aier School of Ophthalmology, Central South University, Changsha, People's Republic of China; [2]Suzhou Institute of Biomedical Engineering and Technology, University of Science and Technology of China, Suzhou, People's Republic of China; [3]Department of Ophthalmology, Second Affiliated Hospital of Anhui Medical University, Hefei, People's Republic of China; [4]Department of Ophthalmology, University of South Florida, Tampa, FL, USA; [5]Shanghai Aier Eye Hospital, Shanghai, People's Republic of China; [6]Department of Ophthalmology, Xiang'an Hospital of Xiamen University, Xiamen University, Xiamen, People's Republic of China; [7]Shanghai Aier Eye Insititute, Shanghai, People's Republic of China

Correspondence: Wensheng Li, Shanghai Aier Eye Hospital, 83 Wuzhong Road, Shanghai, People's Republic of China, Email drlws@qq.com; Shiying Li, Department of Ophthalmology, Xiang'an Hospital of Xiamen University, Xiamen University, Xiamen, People's Republic of China, Email shiying_li@126.com

Purpose: This study aimed to determine the effect and its mechanism of fenofibrate on retinal pigment epithelium (RPE) injury induced by excessive fat in vitro and in vivo.

Methods: ARPE-19 cells were co-incubated with palmitic acid (PA) and fenofibric acid (the active form of fenofibrate after metabolism in vivo) and mice fed with high-fat diet (HFD) were supplemented with fenofibrate. The following methods were used: Western blot and immunofluorescent staining to determine expressions of reactive oxygen species (ROS)–associated factors and proinflammatory cytokines; electroretinogram (ERG) c-wave to evaluate RPE function; TUNEL staining to detect the apoptotic cell in RPE tissue. Additionally, ARPE19 cells were treated with PI3K/AKT inhibitor or agonist to investigate the mechanism of fenofibric acid inhibiting PA-induced RPE damage.

Results: We found that the application of PA inhibited RPE cell viability in a dose-dependent manner, and increased the levels of NAPDH oxidase 4 (NOX4), 3-nitrotyrosin (3-NT), intracellular adhesion molecule-1(ICAM1), tumor necrosis factor alpha (TNFα) and vascular endothelial growth factor (VEGF) at 400μM. The application of fenofibric acid resulted in the inhibition of NOX4, 3-NT, TNFα, ICAM1 and VEGF expression in ARPE-19 cells treated with PA. Moreover, wortmannin, as a selective inhibitor of PI3K/AKT pathway, abolished the effects of fenofibrate on the oxidative stress and inflammation in ARPE-19 cells. In addition, 740Y-P, a selective agonist of PI3K/AKT pathway, enhanced the protective action of fenofibrate. Meanwhile, in vivo dosing of fenofibrate ameliorated the downregulated amplitudes of ERG c-wave in HFD-fed mice and suppressed the HFD-induced oxidative injury and inflammatory response in RPE tissues.

Conclusion: Our results suggested that fenofibrate ameliorated RPE cell damage induced by excessive fat in vitro and in vivo, in part, through activation of the PI3K/AKT signaling pathway.

Keywords: fenofibrate, RPE, palmitic acid, high-fat diet, oxidative stress, inflammation

Introduction

As a part of blood-retinal barrier, retinal pigment epithelium (RPE) integrity is an important factor in maintaining the health and proper functioning of the outer retina. Oxidative stress and local inflammation likely play a role as potential common mechanisms common for retinal diseases.[1–4] Therefore, a study of RPE dysfunction induced by pathogenic factors may have an important role in early prevention and treatment of retinal degeneration.

Lipid homeostasis disruption is considered to be involved in the pathogenesis of retinal diseases, based on finding lipid deposits on the retina, Bruch's membrane and in soft drusen.[5,6] Total and saturated fat consumption may contribute to retinal diseases, but epidemiological evidence is mixed.[7] High-fat diet (HFD) rich in saturated fatty acid (FFAs) have

Received: 6 May 2023
Accepted: 10 November 2023
Published: 21 November 2023

been utilized in rodent models to understand the effect of dietary fat on diabetic retinopathy (DR) and age-related macular degeneration (AMD) and possible mechanisms.[8] Application of HFD led to increased thickness and lipid depositions in Bruch's membrane and impaired RPE integrity in the other disease models.[9,10] However, few studies reported the effects and its mechanism of HFD alone on RPE damage and dysfunction.

Fatty acids are chemically classified as saturated and unsaturated (monounsaturated and polyunsaturated). Saturated FFAs were considered as the key players in the pathogenesis of HFD-enhanced skin inflammation.[11] Palmitic acid (PA) is the most common saturated FFAs present in the diet and in serum.[12] In in vitro cell cultures, PA is widely used to investigate the liopotoxicity effects on non-adipose cells.[13–15] Furthermore, it was shown that PA is present as a major fatty acid in human lipofuscin granules[16] and application of PA induced remarkable cytostatic effect on an RPE cell line (R-50 cells).[17] However, the mechanism of PA alone-induced RPE cells cytotoxicity remained unclear. Therefore, a study of RPE damage in an HFD-fed mice model and a PA-induced cell model, may be helpful to improve our understanding of the complicated relationship between high fat and retinal degeneration.

Fenofibrate is a selective agonist of peroxisome proliferative activated receptor alpha (PPARα) and can promote the β-oxidation of fatty acids.[18] Two large randomized clinical trials, the Fenofibrate Intervention and Event Lowering in Diabetes (FIELD) and the Action to Control Cardiovascular Risk in Diabetes (ACCORD) studies suggest that fenofibrate reduced the progression of diabetic retinopathy.[19,20] Under diabetic conditions, it has been demonstrated that fenofibrate (or fenofibric acid) could prevent the inflammatory process, oxidative stress, angiogenesis, disorganization of tight junction proteins and the hyperpermeability in RPE.[21–27] Above studies focused on investigating the effect of fenofibrate on RPE in the context of diabetic retinopathy. However, rare studies have been published describing a direct effect of fenofibrate on RPE tissue induced by high fat and underlying mechanism. Our study aimed to characterize the effect of fenofibrate on RPE dysfunction and pathological changes from a novel aspect of high fat intake and to illustrate a key mechanism of fenofibrate protecting RPE from the effects of lipid overload.

Materials and Methods

Reagents

Fenofibrate (Feno) and palmitic acid (PA) was purchased from Sigma-Aldrich (St. Louis, MO, USA). Fenofibric acid (FA) and wortmannin were purchased from Abmole (Houston, TX, USA). 740Y-P was purchased from APEXBIO (Houston, TX, USA).

ARPE19 Cells Culture

ARPE19 cells were purchased from Cell resource center, Shanghai Institute of life sciences, Chinese Academy of Sciences (Shanghai, China) and maintained in Dulbecco's modified Eagle's medium F-12 (DMEM/F12) (Invitrogen, Carlsbad, CA, USA) supplemented with 10% heat-inactivated fetal bovine serum (HyClone, Logan, Utah, USA) in a humidified incubator with 5% CO2 at 37°C. The morphology of ARPE-19 cells used in this study was shown in Supplementary Figure 1. Validation of the used ARPE-19 cells with RPE cell-specific markers including Rlbp1 and RPE65 was shown in Supplementary Figure 2.

PA Solution Preparation

PA was dissolved in 0.1 mol/L NaOH and shook in water bath at 75°C for 30 minutes to obtain 40mmol/L PA. This solution was diluted at ratio of 1:1 in preheated 40% (w/v) bovine serum albumin to give a stock PA solution (20 mmol/L PA), which was diluted in supplemented medium to obtain appropriate concentration to use. In vitro, the experimental control group was treated with the vehicle (bovine serum albumin) of 400μM (in Figures 1D-L and 2-4) or 600μM (in Figures 1A-C) palmitic acid in ARPE-19 cells.

Cell Viability Assay

Cell Counting Kit-8 (CCK-8) (Dojindo, Kyushu, Japan) was used to measure the relative cell viability. Briefly, ARPE19 cells (2×10^4 cells/well) were plated in 96-well plates for 24h. After the treatment of PA or FA or vehicle for 24h, CCK8 dilution

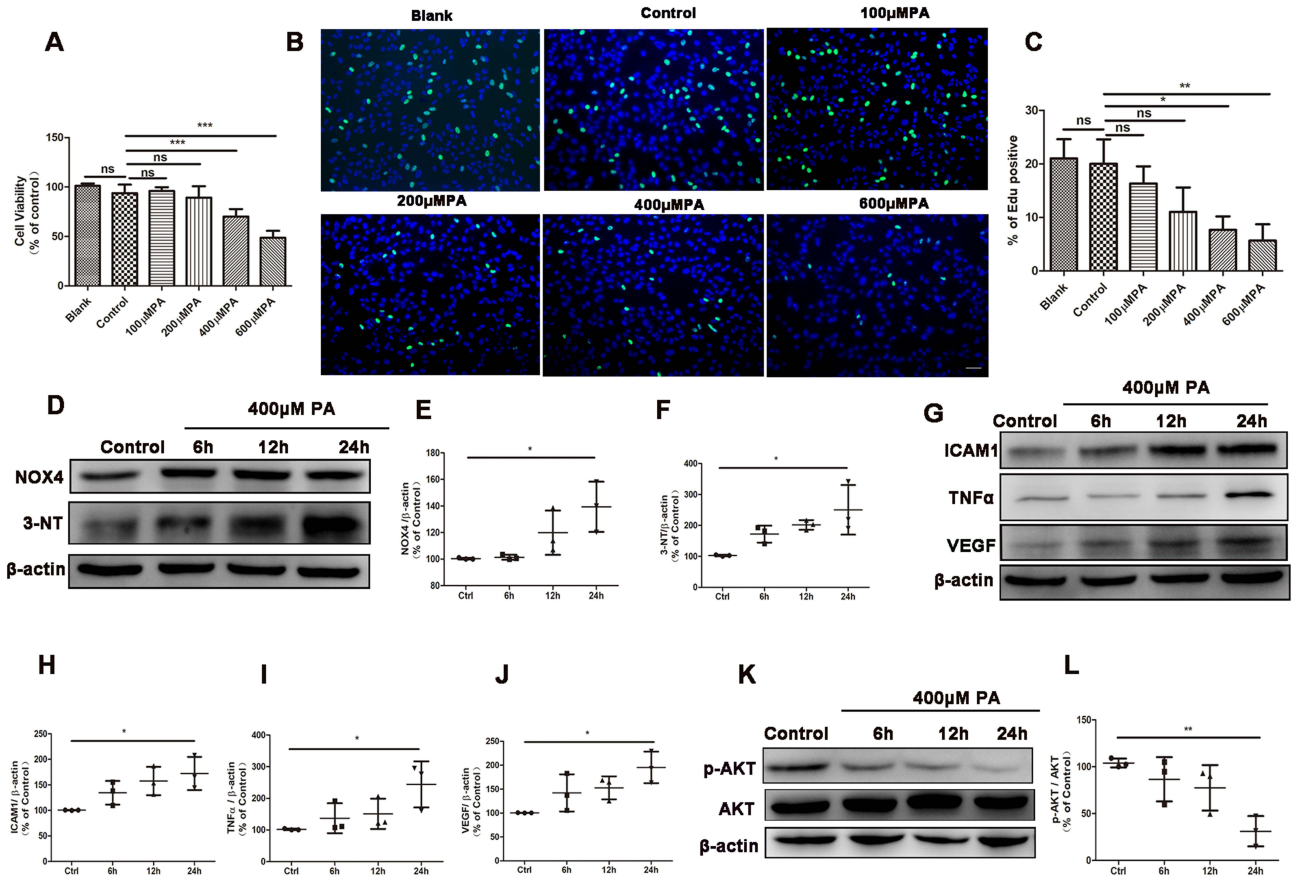

Figure 1 PA induced oxidative stress and inflammation in ARPE19 cells. (**A-C**) Results from cell viability assay (**A**) and EdU staining of cell proliferation (**B** and **C**) in ARPE19 cells treated with nothing (blank group), the vehicle (bovine serum albumin) of 600μM PA (control) or various concentration of PA (100, 200, 400, 600 μM) for 24 hours (Green: EdU, Blue: Hoechest 33,342). Scale bars: 50μm (**B**). (**D**) Representative Western blot images of NOX4, 3-NT in ARPE19 cells treated with vehicle for 24 hours or 400μM PA for 6, 12 and 24 hours. (**E-F**) Analysis of Western blot data of NOX4 and 3-NT. (**G-J**) Images (**G**) and statistical analysis (**H-J**) of Western blot data of ICAM1, TNFα and VEGF levels in ARPE19 cells before and after PA administration. (**K**) Representative images of Western blot of p-AKT and AKT in ARPE19 cells treated with vehicle for 24 hours (control), or 400μM PA for 6, 12 and 24 hours. (**L**) Statistical analysis of Western blot data (**K**) of p-AKT/AKT. Control cells were incubated with the vehicle (bovine serum albumin) of 400μM PA alone for 24 hours (**D-L**). Data were obtained from three independent experiments. One-way analysis of variance (ANOVA) followed by a post-hoc analysis Tukey's test was applied to evaluate significant difference between groups. Bar graphs represent mean values ± SD. *P < 0.05, **P < 0.01, ***P < 0.001.

was added to each well of ARPE-19 cells. The blank well (without ARPE-19 cells) added with only CCK8 dilution was considered as the technical control. After incubation for 4 hours at 37°C in the dark, the absorbance at 450nm was measured with a microplate reader (Thermo Scientific, Carlsbad, CA, USA). The relative cell viability was determined by using the following formula: CV=[(As-Ab)/(Ac-Ab)] *100%, where CV was the relative cell viability, As was the average absorbance of treated cells, Ac was the average absorbance of control cells, Ab was the average absorbance of blank well.

EdU Staining Assay

EdU staining assays were performed using BeyoClick^{TM} EdU Cell Proliferation Kit (Beyotime, Nantong, China). Briefly, ARPE-19 cells were fixed with 4% paraformaldehyde for 1h. After washing with PBS, the cells were incubated with 0.3% TritonX-100 for 20 min. Click additive solution and click reaction solution were prepared according to the manufacturer's instructions, then incubated in the dark for 30 min at room temperature. The staining solution was discarded. ARPE-19 cells were washed with PBS, and incubated with Hoechest 33,342 for 10 min at room temperature for the nuclear staining. After washing with PBS, the positive cells were observed by fluorescence microscopy.

Animal Models

Four-week-old male C57BL/6J mice were purchased from Shanghai Slack Laboratory Animal Co., Ltd., (Shanghai, China). The animals were fed with a standard-fat diet (SD, 10% energy from fat, Research Diets XTCON50J or identified

as D12492, Jiangsu XIETONG Bioengineering Co., Ltd, Nanjing, Jiangsu, China) (n = 15) or high-fat diet (HFD, 60% energy from fat, Research Diets XTHF60 or identified as D12450J, Jiangsu XIETONG Bioengineering Co., Ltd, Nanjing, Jiangsu, China) (n = 15) for 5 months. Compositions of the above two research diets were listed in Supplementary Table 1. Another two groups (n=15/group) were fed the SD or HFD for 5 months and supplemented with 0.1% fenofibrate in the last month. Fenofibrate (Sigma-Aldrich, St. Louis, MO, USA) was dissolved with DMSO (5% w/v) and then well-mixed in the mouse chow to obtain a concentration of 0.1% (w/w) for use. The body weight and body size of mice in the four group was shown in Supplementary Figure 3. All studies were approved by the Experimental Animal Ethics Committee of Suzhou Institute of Biomedical Engineering and Technology, Chinese Academy of Sciences and were performed in accordance with the standards in the Association for Research in Vision and Ophthalmology Statement for the Use of Animals in Ophthalmic and Vision Research.

Western Blot Analysis

After treatment, ARPE19 cells or RPE-choroid-sclera tissues were lysed and the total protein concentrations were determined by BCA protein assay kit (Beyotime, Nantong, China). Equal quantities of protein were resolved by electrophoresis through 10% or 12% tris-glycine SDS polyacrylamide gel and then transferred to a PVDF membrane. The membrane was blocked with 5% (w/v) skim milk in tris-buffered saline containing 0.1%TWEEN-20 (TBST) for 1h or QuickBlock Western blocking buffer (Beyotime, Nantong, China) for 15min at room temperature, subsequently incubated overnight at 4°C with primary antibodies, as listed in Supplementary Table 2. After washing three times (10 min per time) with TBST, the membranes were incubated for 1h at room temperature with an appropriate Horseradish-peroxidase (HRP)-conjugated secondary antibody. The protein bands were detected using a commercial imaging system (ChemiScope 6300; Clinx Science Instrument Co. Ltd, Shanghai, China). The grayscale value of immunoreactive bands were determined via Image J software. We analyzed the differences of the protein expression levels via the comparison of the grayscale ratio of experimental groups vs control group.

Electroretinogram (ERG)

Retinal function was assessed using a visual ERG system (Celeris #D430, Diagnosys, USA). Briefly, mice were dark-adapted at least 12 hours. The animals were anesthetized with inhalation (0.8L/min) of 2% isoflurane for induction phase and then 1.8% isoflurane for maintenance phase. Pupils were dilated with tropicamide/phenylephrine hydrochloride under dim red light. Dark-adapted ERG was performed using flashes with intensities at 0.01, 0.03, 0.1, 0.3, 1.0, 3.0 and 10.0 cd.s/m^2, respectively. For c-wave recording, stimulus was presented for 100 ms with intensities of 150 cd.s/m^2. Responses were averaged and analyzed using the Diagnosys Espion software.

Immunofluorescent Staining

The enucleated mice eyes were fixed in 4% paraformaldehyde for 1h at 4°C and the cornea and lens were removed. The remaining eye cups were transferred successively into 10%, 20% and 30% sucrose solutions for dehydration, and embedded in an OCT compound. Cryosections of eye cups transverse sections were obtained at a thickness of 12μm. The ARPE-19 cells were also fixed in 4% paraformaldehyde for 1h at 4°C. Retinal sections or ARPE-19 cells were incubated in 0.3% Triton X-100 for 20min. After washing with PBS and blocking with 5% normal goat serum, the sections or ARPE-19 cells were incubated with primary antibodies, as listed in Supplementary Table 2, at 4°Covernight and secondary antibodies conjugated with Alexa Fluor® 488 for 1h in the dark at room temperature. Sections were then counterstained with 40, 6-diamidino-2-phenylindole (DAPI) and photographed on a fluorescence microscope.

TUNEL Staining

TUNEL assays were performed on cells or RPE-choroid-sclera flat mounts using the Dead End Fluorometric TUNEL System according to manufacturer's instructions. The flat mounts were co-stained with ZO-1 antibody to confirm the apoptotic cells of RPE tissue. RPE-choroid-sclera flat mounts were then counterstained with DAPI. Images were acquired using the fluorescence microscope (Carl Zeiss Imaging Systems, Oberkochen, Germany).

Statistical Analysis

The statistical analysis was performed with GraphPad Prism v. 5.01 (GraphPad Software, La Jolla, CA). Quantitative data are presented as means ± SD. One-way analysis of variance (ANOVA) followed by a post-hoc analysis Turkey's test or two-way analysis of ANOVA followed by a post-hoc analysis Bonferroni test was applied to evaluate significant difference between groups, and $P < 0.05$ was considered statistically significant.

Results

PA-Induced Oxidative Stress and Inflammation in ARPE-19 Cells

In an in vitro cell model, we investigated the effect of palmitic acid (PA) on oxidative stress and inflammation in ARPE-19 cells. ARPE-19 cells were treated once with vehicle or various concentrations of PA (100, 200, 400, and 600μM) for 24 hours. This resulted in a decrease in cell viability of approximately −2%, 5%, 24% and 45%, respectively (Figure 1A). In the above cell viability tests, 400μM PA was the lowest concentration that resulted in a significant decrease (>30%) in cell viability. In addition, Edu proliferation experiments demonstrated that 400μM and 600μM PA significantly inhibited ARPE-19 cells proliferation (Figures 1B and C). Therefore, ARPE-19 cells were treated with 400μM PA in subsequent experiments.

We then investigated the effect of PA on oxidative stress in ARPE-19 cells. The levels of NAPDH oxidase 4 (NOX4), a key enzyme of ROS generation,[28] and 3-nitrotyrosin (3-NT), a marker of oxidative stress[29] were detected to estimate the level of oxidative injury. Incubation of ARPE19 cells with 400μM PA resulted in a clear increase in the level of NOX4 protein and 3-NT protein at 24 hours (Figure 1D-F). Western blot analysis showed that PA increased pro-inflammatory cytokines intracellular adhesion molecule-1 (ICAM1), tumor necrosis factor alpha (TNFα) and vascular endothelial growth factor (VEGF) at 24 hours compared with control group (Figure 1G-J). Taken together, these findings indicated that the application of PA induced oxidative stress and inflammation in ARPE19 cells.

PI3K/AKT signaling pathway plays an important role in cellular oxidative stress and inflammation.[30,31] Therefore, we then investigated whether PI3K/AKT signaling pathway was involved in the process of ARPE19 cell damage induced by PA. After PA treatment for 0–24 hours, the protein expression of p-AKT and AKT were analyzed by Western blot. We found that the p-AKT/AKT levels significantly decreased after PA treatment at 24 hours (Figures 1K and L), suggesting the involvement of p-AKT/AKT in PA-induced ARPE-19 injury.

Fenofibric Acid Inhibited PA-Induced ARPE-19 Injury

Here, we investigated the effect of fenofibrate on the PA-induced ARPE-19 injury. Fenofibric acid (FA), as an active form of fenofibrate after metabolism in vivo, was used as a substitute for fenofibrate in in vitro experiments.[32,33] Therefore, ARPE-19 cells were treated for 24 hours with 400μM PA in the absence or presence of various concentrations of FA. Edu staining analysis (Figures 2A and B) demonstrated that 20μM and 50μM FA significantly promoted the ARPE-19 cells proliferation, which was consistent with the result of cell viability in CCK8 assay (Figure 2C). We determined the changes of 3-NT and NOX4 after treatment of FA in PA-induced oxidant injury in ARPE19 cells. As shown by the Western blot analysis in Figures 2D-F, FA at the lowest concentration of 20μM significantly suppressed the increased levels of NOX4 and 3-NT induced by PA. Immunostaining analysis showed FA significantly inhibited 3-NT upregulation induced by PA from the concentrations of 20μM to 50μM (Figure 2D and Supplementary Figure 4A). To further verify if the inflammatory response was inhibited by FA in the ARPE19 cells after exposure to PA, we determined the protein levels of the inflammatory cytokines ICAM1, TNFα and VEGF. As shown in Figures 2H-J, the ICAM1 and TNFα upregulations induced with PA were effectively decreased by FA treatment from the concentrations of 20μM. In addition, VEGF expression level in the PA-treated group was markedly inhibited by FA at the concentrations from 10μM to 50μM (Figures 2H and K). Immunostaining analysis also demonstrated FA significantly inhibited PA-induced upregulation of TNFα and VEGF (Figures 2L and M and Supplementary Figures 4B and C). Collectively, these findings indicated that FA alleviated ARPE19 cells injury induced by PA via regulations of oxidative stress and inflammation.

Numerous studies have demonstrated that many drugs or nutritional products with anti-oxidant and anti-inflammatory activities could regulate PI3K/AKT signaling pathway.[34,35] We then investigated whether PI3K/AKT signaling pathway

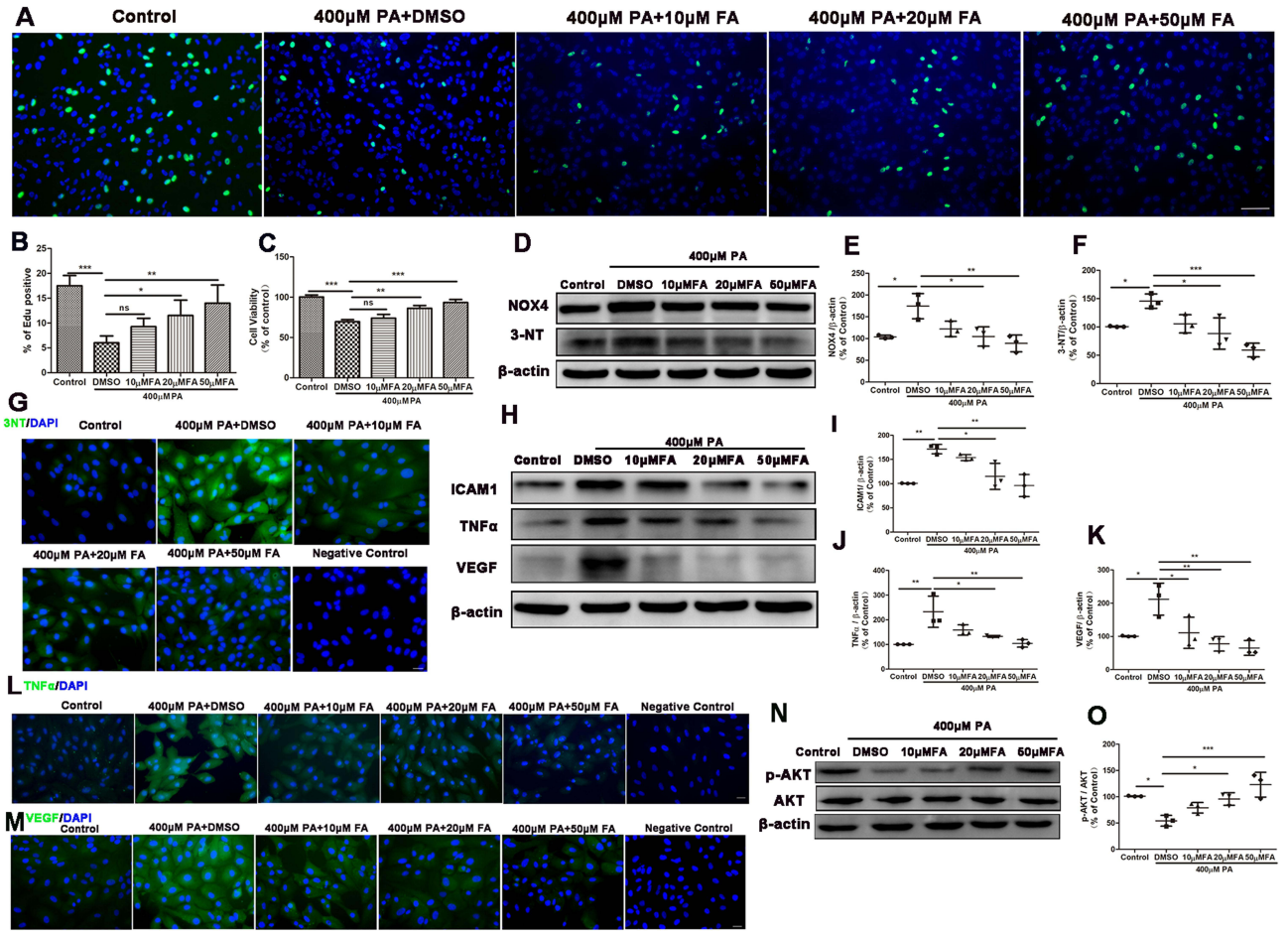

Figure 2 Fenofibric acid (FA) inhibited ARPE19 cells injury induced by PA. ARPE19 cells treated with 400μM PA and DMSO or various concentrations of FA (0, 10, 20, 50μM) for 24 hours. Note that cells were treated with DMSO or FA 1 hour after the initiation of PA-induction. Cells incubated with the vehicle (bovine serum albumin) of 400μM PA alone for 24 hours served as a control. (**A-B**) Edu staining of cell proliferation (**A**) and its statistical analysis of (**B**) (Green: EdU, Blue: Hoechest 33,342). Scale bars: 50μm (**A**). (**C**) CCK8 analysis of cell viability. (**D-F**) Western blot analyses of NOX4 (**D** and **E**), 3-NT (**D** and **F**). (**G**) Immunofluorescence staining of 3-NT in ARPE-19 cells. Scale bars: 50μm (**L**). (**H-K**) Western blot analyses of ICAM1 (**H** and **I**), TNFα (**H** and **J**) and VEGF (**H** and **K**) in ARPE19 cells. (**L-M**) Immunofluorescence staining of TNFα (**L**) and VEGF (**M**) in ARPE-19 cells. Scale bars: 50μm (**L-M**). (**N-O**) Representative images of Western blot of p-AKT and AKT in ARPE19 cells. (**O**) Statistical analysis of Western blot data (**N**) of p-AKT/AKT. Data were obtained from three independent experiments. One-way analysis of variance (ANOVA) followed by a post-hoc analysis Tukey's test was applied to evaluate significant difference between groups. Bar graphs represent mean values ± SD. *P < 0.05, **P < 0.01, ***P < 0.001.

was associated with the process in which FA protected against ARPE-19 cell damage induced by PA. Western blot analysis indicated that the decreased p-AKT/AKT level induced by PA recovered significantly upon FA treatment at a concentration from 20μM to 50μM (Figures 2N and O). The data showed that FA ameliorated PA-induced inhibition of p-AKT/AKT in ARPE-19 cells.

Suppression of PI3K/AKT Pathway Prevented the Ameliorative Effect of Fenofibric Acid (FA) on ARPE-19 Injury

Next, we investigated the role of PI3K/AKT signaling in FA ameliorating ARPE19 cells injury induced by PA. Prior to treatment with 400μM PA and 50μM FA, ARPE-19 cells were incubated with PI3K/AKT inhibitor wortmannin (0, 100, 200, 400nM) for 1 hour. As shown in Figures 3A and B, wortmannin significantly inhibited the upregulation of p-AKT/AKT after FA treatment in a concentration-dependent manner. In addition, we found that the positive effect of FA on oxidative stress was weakened after treatment with PI3K/AKT inhibitor (wortmannin) in a concentration-dependent manner (Figure 3C-E). Similarly, the effect of FA as an inhibitor of the inflammatory response as noted by suppression of ICAM1, TNFα and VEGF was attenuated by the PI3K/AKT inhibitor in a concentration-dependent manner (Figures 3F-I). Together,

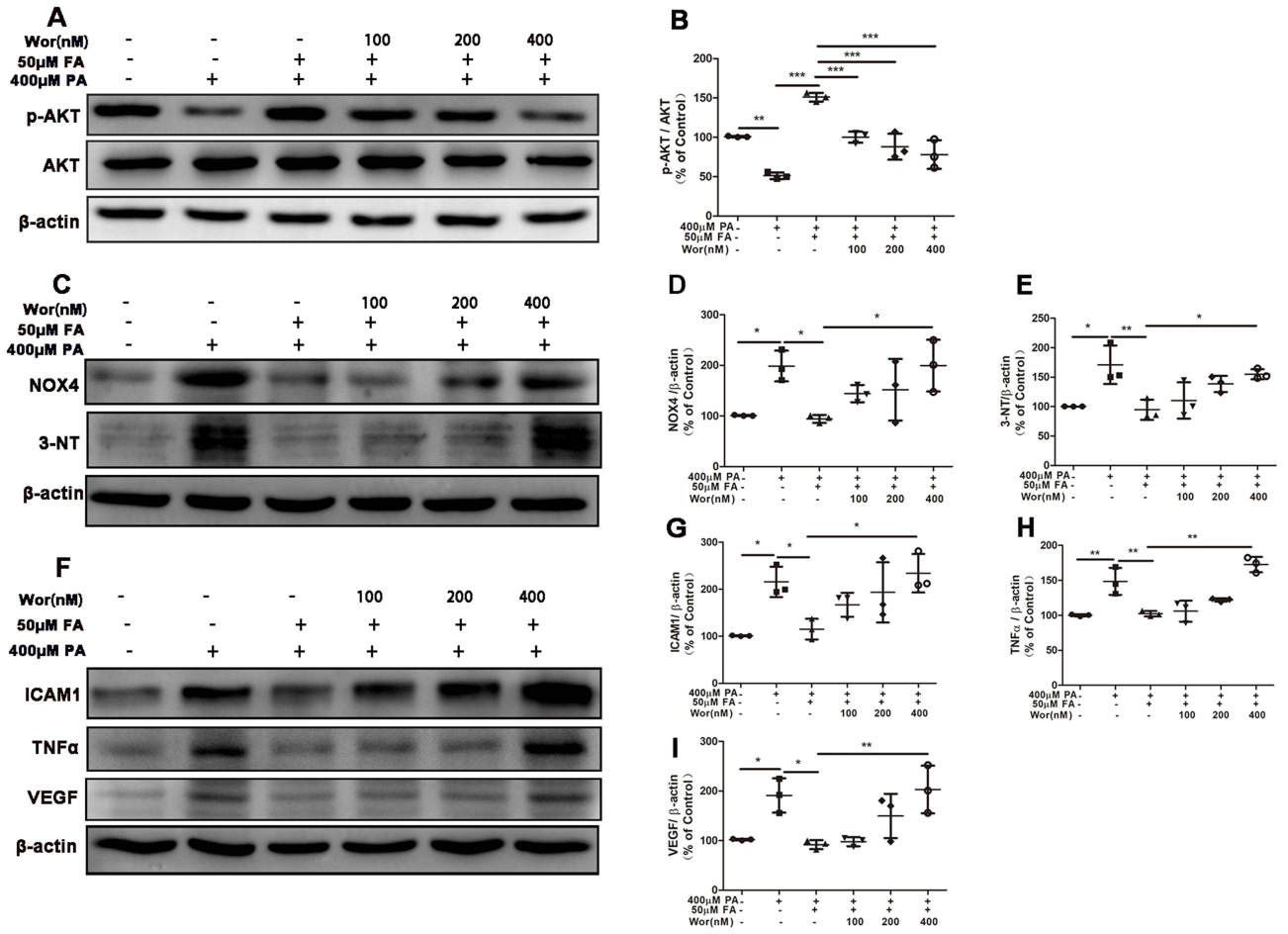

Figure 3 Suppression of PI3K/AKT pathway prevented the ameliorative effect of fenofibric acid (FA) on ARPE-19 cells injury. ARPE-19 cells were pre-treated with various concentrations of wortmannin (0, 100, 200, 400nM) for 1 hour, and then exposed to 400μM PA with or without 50μM FA for 24 hours. (**A**) Representative images of Western blot of p-AKTand AKT levels; (**B**) Statistical analysis of data (**A**) of p-AKT/AKT. (**C**) Representative images of Western blot of NOX4 and 3-NT levels; (**D** and **E**) Statistical analysis of the data presented in C. (**F**) Representative images of Western blot of ICAM1, TNFα and VEGF; (**G-I**) statistical analysis of the data presented in F. Note that cells were treated with FA 1 hour after the initiation of PA-induction. Data were obtained from three independent experiments. One-way analysis of variance (ANOVA) followed by a post-hoc analysis Tukey's test was applied to evaluate significant difference between groups. Bar graphs represent mean values ± SD. *P < 0.05, **P < 0.01, ***P < 0.001.

these results indicated that the suppression of PI3K/AKT signaling pathway prevented the ameliorative effect of FA on PA-induced ARPE-19 cells injury.

Activation of PI3K/AKT Pathway Strengthened the Positive Effect of Fenofibric Acid (FA) on ARPE-19 Injury

ARPE-19 cells were pre-treated with 20μM PI3K/AKT agonist 740 Y-P for 1 hour, and then incubated with 400μM PA and 20μM FA. Western blot analyses showed that p-AKT/AKT upregulation induced by FA was further elevated significantly by 740Y-P treatment (Figures 4A and B). We also found that the alleviation of oxidative stress (measured by NOX4 and 3-NT) induced by FA was significantly enhanced upon treatment with 740Y-P (Figures 4C-E). Consistently, the levels of inflammatory factors ICAM1, TNFα and VEGF were significantly inhibited by the application of FA, and this process was further enhanced by 740 Y-P (Figures 4F-I). These results suggested that PI3K/AKT activation increased the inhibitory effects of FA on oxidative stress and inflammation induced by PA.

Fenofibrate Ameliorated HFD-Induced Retinal Dysfunction

We then investigated the effect of fenofibrate on the HFD-induced RPE injury in vivo, mice were fed with 0.1% fenofibrate, which was added in their diet in the last month of high-fat diet regimen. High-intensity ERG flash stimulation was applied, and an evaluation of the c-wave was performed to estimate the effect of HFD and fenofibrate on the functioning of RPE. After HFD

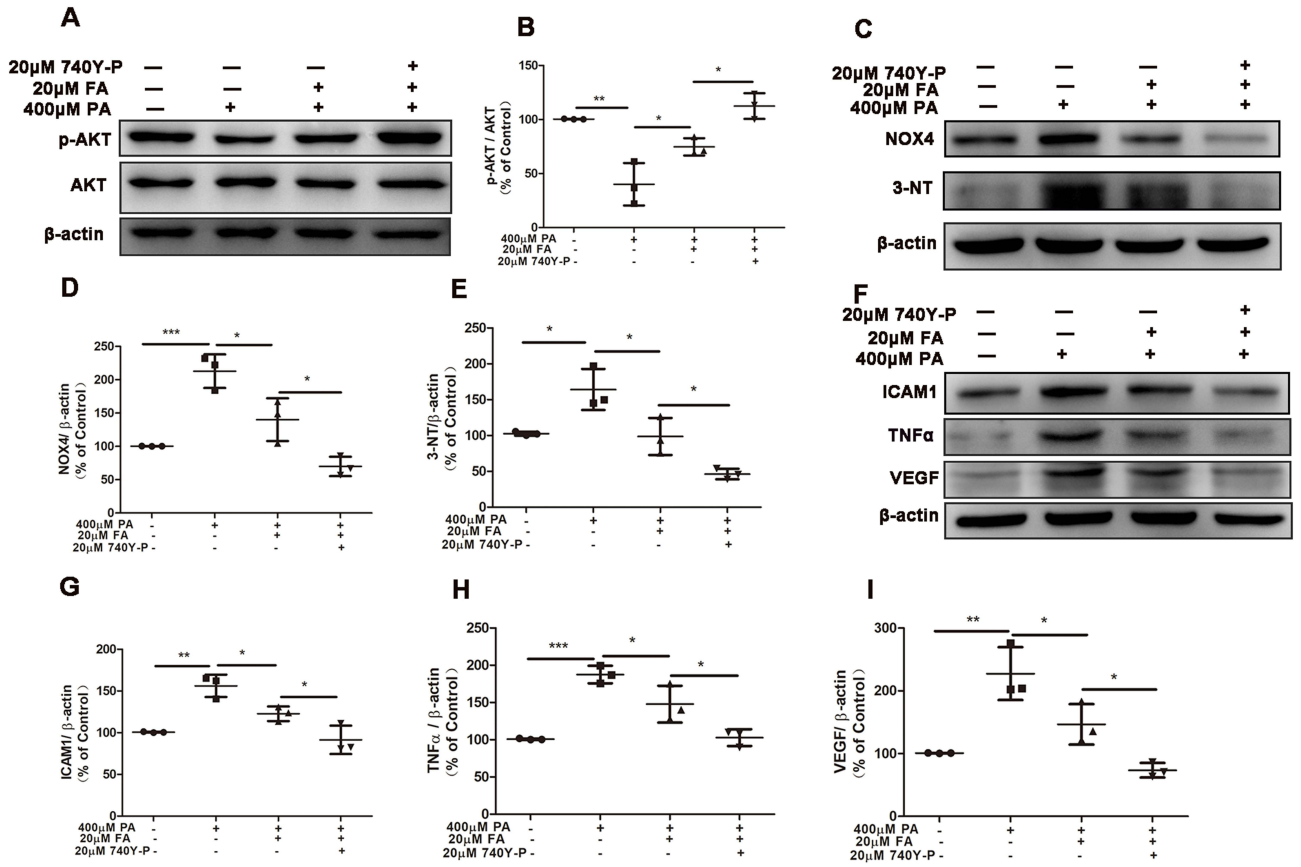

Figure 4 Activation of PI3K/AKT pathway strengthened the alleviation of fenofibric acid (FA) in ARPE-19 cells injury. ARPE-19 cells were pre-treated with 20μM 740Y-P for 1 hour, and then exposed to 400μM PA with or without 20μM FA for 24 hours. (**A**) Representative images of Western blot of p-AKT and AKT levels; (**B**) Statistical analysis of data (**A**) of p-AKT/AKT. (**C**) Representative images of Western blot of NOX4 and 3-NT levels; (**D** and **E**) Statistical analysis of the data presented in C. (**F**) Representative images of Western blot of ICAM1, TNFα and VEGF; (**G-I**) statistical analysis of the data presented in F. Note that cells were treated with FA 1 hour after the initiation of PA-induction. Data were obtained from three independent experiments. One-way analysis of variance (ANOVA) followed by a post-hoc analysis Tukey's test was applied to evaluate significant difference between groups. Bar graphs represent mean values ± SD. *P < 0.05, **P < 0.01, ***P < 0.001.

feeding for 5 months, the c-wave amplitudes (at 150cd.s/m^2 stimulus luminance) were 51.9% of those in SD-fed mice (Figures 5A and B). Fenofibrate treatment partially (by ~33.6%) reversed the decreased amplitudes of ERG c-wave in the HFD mice (Figures 5A and B). In an additional analysis, we also evaluated the changes in ERG a- and b-waves, which reflect the bioelectrical activity of photoreceptors and bipolar cells in the retina. As shown in Supplementary Figure 5, HFD for 5 months significantly reduced a-wave (by ~46.9%) and b-wave (by ~48.6%) amplitudes under scotopic conditions at the light stimulates of 10cd.s/m^2, which were partially reversed by fenofibrate supplementation (by ~20% in a-wave and ~23% in b-wave). These results indicated that fenofibrate treatment significantly ameliorated HFD-induced RPE and neuroretina dysfunction.

Fenofibrate Ameliorated RPE Injury Induced by HFD in Mice

We next examined the effect of HFD and fenofibrate on the pathological changes in RPE tissue. RPE-choroid-sclera flat mounts showed that fenofibrate supplementation reversed the HFD-induced increase in the percentage of TUNEL staining positive cells (Figures 6A and B), which indicated fenofibrate had a protective effect on HFD-induced apoptosis cells of RPE tissue. Subsequently, we further evaluated the effect of HFD and fenofibrate on the oxidative stress and inflammation in RPE tissue. Western blot analyses indicated that HFD triggered oxidative stress and an inflammatory response, because the expression level of oxidative stress markers (such as: 3-NT, 4-HNE) (Figures 6C-E) and proinflammatory cytokines (such as: ICAM1, TNFα and VEGF) (Figures 6G-J) dramatically increased in RPE-choroid-sclera tissues of HFD-fed mice. Fenofibrate treatment significantly reduced 3-NT and 4-HNE protein (Figures 6C-E), as well as ICAM1, TNFα and VEGF protein expression levels (Figures 6G-J). Immunostaining showed that NOX4 and TNFα increased significantly in RPE tissue after a 5-month HFD, and fenofibrate treatment down-regulated the

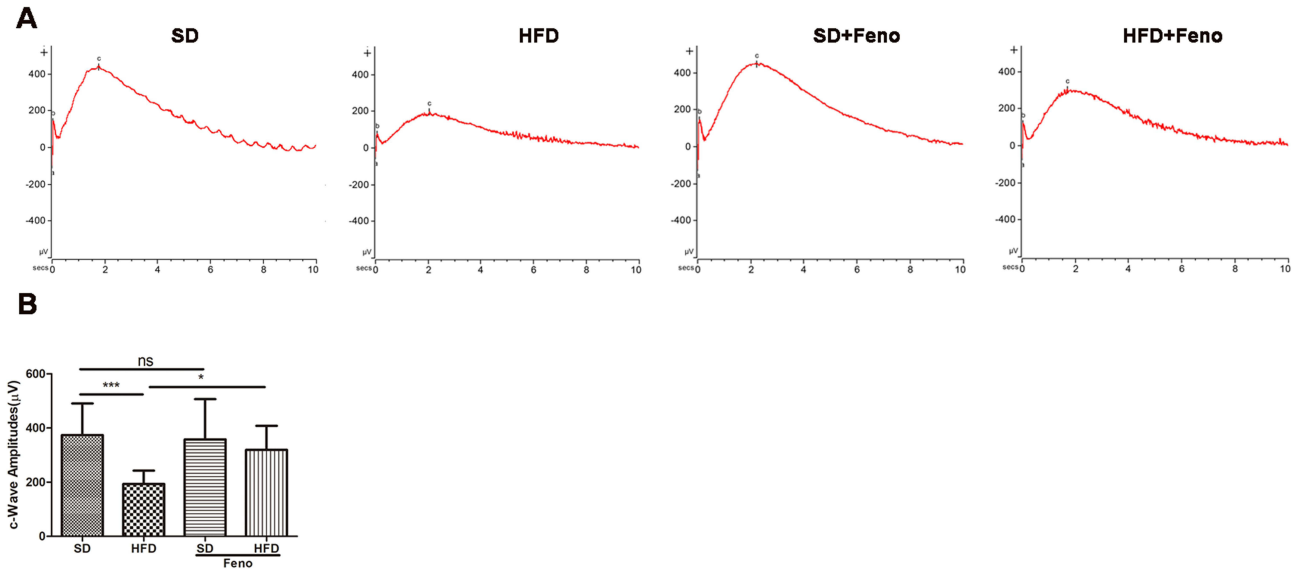

Figure 5 Fenofibrate ameliorated HFD-induced RPE dysfunction. Mice were fed with HFD for 5 mouths and supplemented with 0.1% fenofibrate (Feno) in their diet in the last month. (**A**) Representative electroretinogram (ERG) c-wave for four groups in response to a light stimulation intensity of 150.0 cd.s/m2 under scotopic conditions. (**B**) Statistical analysis of amplitude changes of ERG c-wave under stimulus intensities of 150.0 cd.s/m2 under scotopic conditions. n=13 (SD), 12 (HFD), 14 (SD_ Fe), 11 (HFD_ Fe). One-way analysis of variance (ANOVA) followed by a post-hoc analysis Tukey's test was applied to evaluate significant difference between groups. Bar graphs represent mean values ± SD. ns: not significant, *P < 0.05, ***P < 0.001.

expression of NOX4 (a biomarker of oxidative stress) (Figures 6F and Supplementary Figure 6A) and TNFα (Figures 6K and Supplementary Figure 6B) in RPE tissue. These results suggested fenofibrate treatment ameliorated the level of oxidative stress and inflammatory activity in RPE cells induced by HFD in mice.

Therefore, we further determined the expression of p-AKT and AKT in RPE-choroid-sclera tissues of mice. The Western blot analysis showed that the ratio of p-AKT/AKT were downregulated after 5 months of HFD feeding, and fenofibrate supplementation significantly inhibited the decreased level of p-AKT/AKT (Figure 6L and M). These results indicated that fenofibrate could reduce the inhibition of p-AKT/AKT in RPE-choroid-sclera tissues of HFD-fed mice.

Discussion

We provided novel evidence demonstrating antioxidant and anti-inflammatory effects of fenofibrate on RPE, using RPE injury model induced by excessive fat in vitro and in vivo. These results are consistent with our previous finding that fenofibrate has anti-inflammatory effects against retinal inflammation induced by HFD.[36] The current study also demonstrated that the one of the underlying mechanisms of fenofibrate protection of the RPE is via the activation of the PI3K/AKT signaling pathway.

Free fatty acids (FFAs), including palmitic acid (PA) and oleic acid (OA), have been considered as the two main compositions in lipofuscin.[16] Saturated PA has been widely used in in vitro cell cultures to induce DNA damage and generate genotoxicity in insulin-secreting cells.[37] However, monounsaturated OA was reported to protect pancreatic cells against PA-induced apoptosis.[38] In the RPE, unsaturated OA may enhance autophagy flux, but did not induce apoptotic cell death signal.[17] Autophagy flux is thought to play a cytoprotective role against various external insults, and inhibition of autophagy flux could induce RPE cell death.[39] Conversely, oxidative stress and inflammation have both physiological and potentially pathological roles in RPE degeneration.[40] Recent study reported that saturated PA could aggravate high glucose-induced inflammatory response in ARPE-19 cells.[41] Therefore, we speculated that saturated PA may play a critical role in RPE degeneration. In the current study, we demonstrated that the direct application of saturated PA on RPE cells for 24 hours results in RPE damage by activation of oxidative stress and inflammatory response in an in vitro model.

In vivo, the effect of dietary fat on the retinal function and structure has recently become a popular topic.[42] However, very few studies have reported the effect of HFD alone on the RPE tissue. Recent study found that RPE thickness and

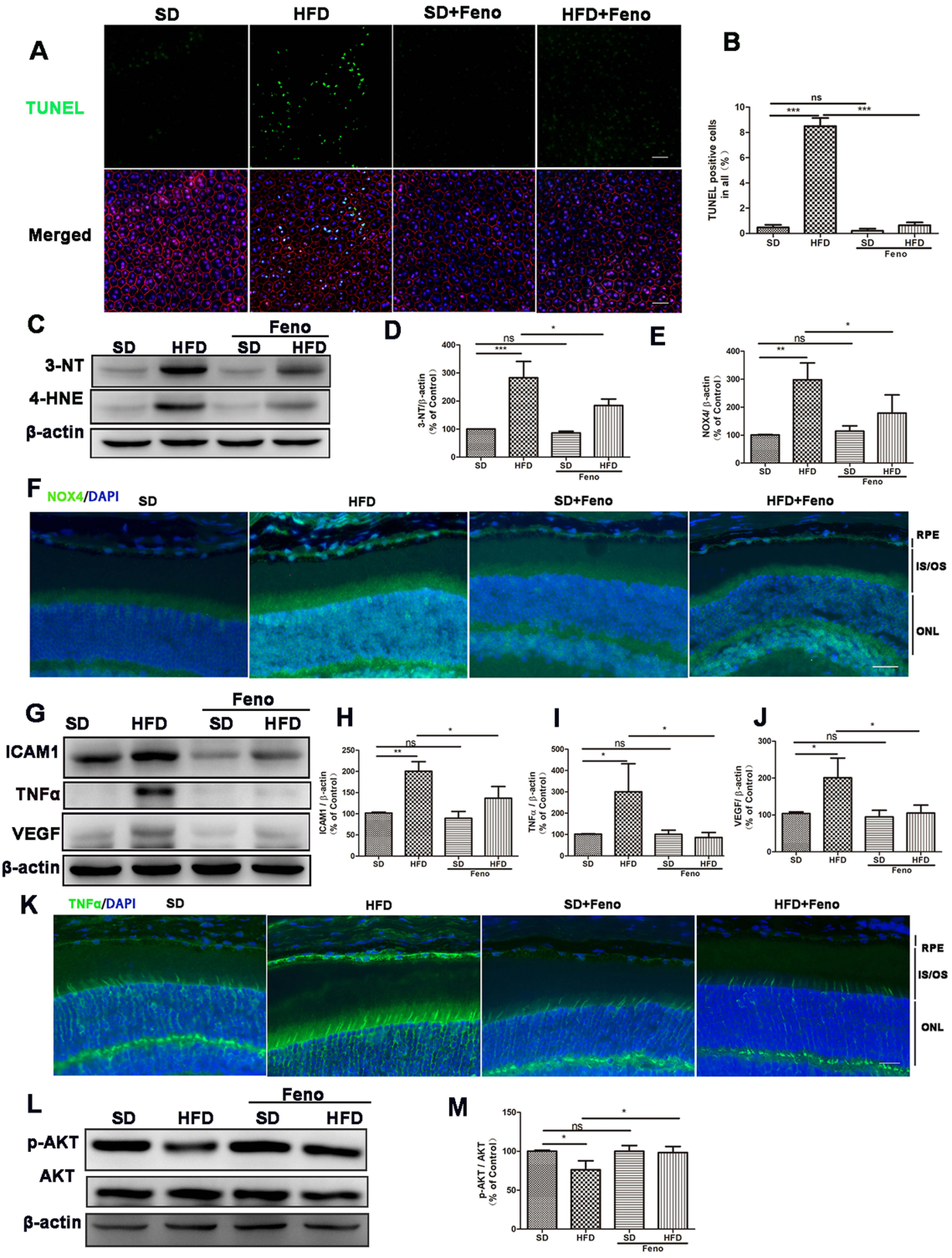

Figure 6 Fenofibrate ameliorated RPE injury induced by HFD in mice. Mice were fed with HFD for 5 mouths and supplemented with 0.1% fenofibrate (Feno) in their diet in the last month. (**A**) Representative images of TUNEL staining of mice RPE tissue (Green: TUNEL, Red: ZO-1, Blue: DAPI). (**B**) Statistical analysis of the percentage of TUNEL positive cells relative to the total number of cells in the images shown in Figure 6A. (**C**) Representative images of Western blot of 3-NT and 4-HNE protein levels in RPE-choroid-sclera tissues. (**D-E**) Statistical analysis of the data presented in C. (**F**) Representative images of immunofluorescence staining of ROS marker NOX4 of mice RPE tissue. (Green: NOX4, Blue: DAPI). (**G**) Representative images Western blot protein levels of ICAM1, TNFα and VEGF in RPE-choroid-sclera. (**H-J**) Statistical analysis of the data presented in (**G**). (**K**) Representative images of immunofluorescence staining of pro-inflammatory cytokine TNFα of mice RPE tissue. (Green: TNFα, Blue: DAPI). (**L**) Representative images of Western blot of p-AKT and AKT protein levels in RPE-choroid-sclera tissues. (**M**) Statistical analysis of the data (**L**) of p-AKT/AKT. Scale bars: 50μm (**A, F** and **K**). One-way analysis of variance (ANOVA) followed by a post-hoc analysis Tukey's test was applied to evaluate significant difference between groups. Bar graphs represent mean values ± SD. n=5, ns: not significant, *P < 0.05, **P < 0.01, ***P < 0.001.

retinal function (measured by ERG a-wave and b-wave) did not deteriorate, however, AMD-linked proteins clusterin and TIMP3 accumulated in the RPE and Bruch's membrane of mice fed with 45% HFD for 12 months.[43] In contrast, another study demonstrated that application of 60% HFD impaired retinal function after 6 months.[44] In the present study, we revealed that administration of 60% HFD for 5 months significantly decreased the ERG a-, b- and c-wave amplitude. This finding suggested that retinal and RPE dysfunction occurred in mice at 5 months of 60% HFD feeding. In addition, our study also demonstrated that 60% HFD for 5 months was responsible for pathological damage (including apoptosis, oxidative stress and inflammation) in RPE.

Fenofibrate (as a PPARα agonist) exerted its beneficial effects on retina in a PPARα-dependent or independent mechanisms. Chen et al supported that fenofibrate attenuated retinal vascular leakage in a streptozotocin-induced diabetic rat model via activation of PPARα.[45] Inconsistently, it was reported that fenofibrate prevented human retinal endothelial cells death induced by serum deprivation through a PPARα-independent manner.[46] Besides, fenofibric acid also alleviate RPE barrier impairment induced by heavily oxidized, glycated low-density lipoprotein through a PPARα-independent mechanism.[27] However, it was unclear what the effect of fenofibrate on high fat-induced RPE damage would be and which underlying mechanism would be involved. In the current study, supplementing the HFD with fenofibrate partially reversed the inhibited amplitudes of ERG c-wave, and also reversed the increased oxidative stress levels and proinflammatory cytokines in RPE tissue in vivo. Furthermore, fenofibric acid reduced the levels of reactive oxygen species and proinflammatory cytokines in ARPE-19 cells induced by PA.

In terms of mechanism, the difference between two research diets was the proportion of fatty acid, especially the proportion of lard abundant with saturated FFAs (Supplementary Table 1). HFD rich in saturated FFAs might not stimulate the PPARα-mediated fatty acid-β-oxidation because PPARα natural ligands are omega-3 polyunsaturated fatty acid (PUFA).[47] In addition, high-throughput real-time PCR showed that PA (known as saturated FFAs) alone did not alter the expression of PPARα in HepG2 cells.[48] Taken together, PPARα might not be a target for RPE injury induced by high saturated FFAs. Therefore, we speculated that fenofibrate inhibited RPE injury induced by HFD or PA in a PPARα-independent manner.

AKT, as a protein kinase downstream of PI3K, regulated lipid and glucose metabolism.[49] Previous study has reported that PA inhibited PI3K/AKT signaling, which is associated with the reduction of glucose uptake in HepG2 cells.[50] Consistently, in this study, high fat significantly suppressed AKT phosphorylation in ARPE19 cell and RPE tissue. In addition, PI3K/AKT signaling pathway has been evidenced to be involved in alleviating oxidative stress in the retina and ARPE19 cells.[51–53] Our study further investigated whether PI3K/AKT signaling, by introducing PI3K/AKT inhibitor or agonist, was the target for the protective effect of fenofibrate on RPE injury induced by high fat. Our data showed that inhibition of PI3K/AKT signaling reduced the protective effects of fenofibrate on oxidative stress and inflammation. In addition, PI3K/AKT signaling activated by 740Y-P promoted the inhibition of oxidative stress and inflammation. These findings indicate that at least one essential mechanism by which fenofibrate prevents from RPE injury induced by high fat is through activation of the PI3K/AKT signaling pathway.

Our work has some limitations. Firstly, ARPE-19 cells were limited in aspect of assessment of the pharmacology data compared with primary RPE cells. Secondly, we did not control the daily intake of research diet and fenofibrate. Finally, the full scope of fenofibrate RPE protective action, likely through various lipid metabolism changes, remains elusive. Future studies are warranted in order to reveal the multitude of underlining mechanisms.

Conclusions

In conclusion, our results indicated that high fat likely induced RPE damage, as indicated by the results of PA-induced cell model and HFD-induced animal model. Furthermore, fenofibrate was able to protect against RPE injury induced by high fat via the activation of PI3K/AKT signaling pathway. Overall, these findings would contribute to our understanding of the pathophysiology associated with the effect of dietary lipids on RPE health and points to potential treatment strategies for retinal degenerative diseases.

Data Availability

Data is contained within the article or the Supplemental Material.

Ethics Statement

The mice experimentation protocol was approved by the Experimental Animal Ethics Committee of Suzhou Institute of Biomedical Engineering and Technology, Chinese Academy of Sciences under permit number SIBET-2019-B20.

Acknowledgments

The authors thank C. H. Dong and T. K. Yuan for their technical supports. In addition, we thank staffs from the Advanced Optical Micro-Imaging Platform of Suzhou Institute of Biomedical Engineering and Technology, China Academy of Science for their assistance with imaging experiments.

Author Contributions

All authors made a significant contribution to the work reported, whether that is in the conception, study design, execution, acquisition of data, analysis and interpretation, or in all these areas; took part in drafting, revising or critically reviewing the article; gave final approval of the version to be published; have agreed on the journal to which the article has been submitted; and agree to be accountable for all aspects of the work.

Funding

This work was supported by the Science Research Fundation of Aier Eye Hospital Group (AR2201D3 [J. S. Yang]) and Clinical-Basic Joint PI Research Project of Aier Eye Institute (LCERI-001 [W. S. Li]).

Disclosure

The authors report no conflicts of interest in this work.

References

1. Nowak JZ. Age-related macular degeneration (AMD): pathogenesis and therapy. *Pharmacol Rep*. 2006;58(3):353–363.
2. Cunnusamy K, Ufret-Vincenty R, Wang S. Next-generation therapeutic solutions for age-related macular degeneration. *Pharm Patent Analyst*. 2012;1(2):193–206. doi:10.4155/ppa.12.12
3. Marfany G. The Relevance of Oxidative Stress in the Pathogenesis and Therapy of Retinal Dystrophies. *Antioxidants*. 2020;9.
4. Ruan Y, Jiang S, Musayeva A, Gericke A. Oxidative Stress and Vascular Dysfunction in the Retina: therapeutic Strategies. *Antioxidants*. 2020;9.
5. Meng LH, Chen YX. Lipid accumulation and protein modifications of Bruch's membrane in age-related macular degeneration. *Int J Ophthalmol*. 2021;14:766–773. doi:10.18240/ijo.2021.05.19
6. Wang Y, Liu Y, Liu S, et al. A novel and efficient murine model of Bietti crystalline dystrophy. *Dis Model Mech*. 2022;15.
7. van Leeuwen EM, Emri E, Merle BMJ, et al. A new perspective on lipid research in age-related macular degeneration. *Prog Retin Eye Res*. 2018;67:56–86. doi:10.1016/j.preteyeres.2018.04.006
8. Clarkson-Townsend DA, Douglass AJ, Singh A, Allen RS, Uwaifo IN, Pardue MT. Impacts of high fat diet on ocular outcomes in rodent models of visual disease. *Exp Eye Res*. 2021;204:108440. doi:10.1016/j.exer.2021.108440
9. Zhang M, Chu Y, Mowery J, et al. Pgc-1α repression and high-fat diet induce age-related macular degeneration-like phenotypes in mice. *Dis Model Mech*. 2018;11.
10. Zhao Z, Xu P, Jie Z, et al. γδ T cells as a major source of IL-17 production during age-dependent RPE degeneration. *Invest Ophthalmol Vis Sci*. 2014;55(10):6580–6589. doi:10.1167/iovs.14-15166
11. Herbert D, Franz S, Popkova Y, et al. High-Fat Diet Exacerbates Early Psoriatic Skin Inflammation Independent of Obesity: saturated Fatty Acids as Key Players. *J Invest Dermatol*. 2018;138(9):1999–2009. doi:10.1016/j.jid.2018.03.1522
12. Baylin A, Kabagambe EK, Siles X, Campos H. Adipose tissue biomarkers of fatty acid intake. *Am J Clin Nutr*. 2002;76(4):750–757. doi:10.1093/ajcn/76.4.750
13. Yang L, Guan G, Lei L, Liu J, Cao L, Wang X. Oxidative and endoplasmic reticulum stresses are involved in palmitic acid-induced H9c2 cell apoptosis. *Biosci Rep*. 2019;39.
14. Ohtsubo K, Chen MZ, Olefsky JM, Marth JD. Pathway to diabetes through attenuation of pancreatic beta cell glycosylation and glucose transport. *Nat Med*. 2011;17(9):1067–1075. doi:10.1038/nm.2414
15. Sun Y, Yang J, Liu W, et al. Attenuating effect of silibinin on palmitic acid-induced apoptosis and mitochondrial dysfunction in pancreatic β-cells is mediated by estrogen receptor alpha. *Mol Cell Biochem*. 2019;460(1–2):81–92. doi:10.1007/s11010-019-03572-1
16. Bazan HE, Bazan NG, Feeney-Burns L, Berman ER. Lipids in human lipofuscin-enriched subcellular fractions of two age populations. Comparison with rod outer segments and neural retina. *Invest Ophthalmol Vis Sci*. 1990;31:1433–1443.
17. Chang YC, Lin CW, Chang YS, et al. Monounsaturated oleic acid modulates autophagy flux and upregulates angiogenic factor production in human retinal pigment epithelial ARPE-19 cells. *Life Sci*. 2020;259:118391. doi:10.1016/j.lfs.2020.118391
18. Guay DR. Update on fenofibrate. *Cardiovasc Drug Rev*. 2002;20(4):281–302. doi:10.1111/j.1527-3466.2002.tb00098.x
19. Keech AC, Mitchell P, Summanen PA, et al. Effect of fenofibrate on the need for laser treatment for diabetic retinopathy (FIELD study): a randomised controlled trial. *Lancet*. 2007;370(9600):1687–1697. doi:10.1016/S0140-6736(07)61607-9

20. Chew EY, Ambrosius WT, Davis MD, et al. Effects of medical therapies on retinopathy progression in type 2 diabetes. *N Engl J Med*. 2010;363:233–244.
21. Trudeau K, Roy S, Guo W, et al. Fenofibric acid reduces fibronectin and collagen type IV overexpression in human retinal pigment epithelial cells grown in conditions mimicking the diabetic milieu: functional implications in retinal permeability. *Invest Ophthalmol Vis Sci*. 2011;52 (9):6348–6354. doi:10.1167/iovs.11-7282
22. Villarroel M, Garcia-Ramirez M, Corraliza L, Hernandez C, Simo R. Fenofibric acid prevents retinal pigment epithelium disruption induced by interleukin-1 beta by suppressing AMP-activated protein kinase (AMPK) activation. *Diabetologia*. 2011;54(6):1543–1553. doi:10.1007/s00125-011-2089-5
23. Miranda S, Gonzalez-Rodriguez A, Garcia-Ramirez M, et al. Beneficial effects of fenofibrate in retinal pigment epithelium by the modulation of stress and survival signaling under diabetic conditions. *J Cell Physiol*. 2012;227(6):2352–2362. doi:10.1002/jcp.22970
24. Garcia-Ramirez M, Hernandez C, Palomer X, Vazquez-Carrera M, Simo R. Fenofibrate prevents the disruption of the outer blood retinal barrier through downregulation of NF-kappa B activity. *Acta Diabetol*. 2016;53(1):109–118. doi:10.1007/s00592-015-0759-3
25. Farris RA, Price ET. Reverse Translational Study of Fenofibrate's Observed Effects in Diabetes-Associated Retinopathy. *Clin Transl Sci*. 2017;10 (2):110–116. doi:10.1111/cts.12412
26. Liu Q, Zhang X, Cheng R, Ma JX, Yi J, Li J. Salutary effect of fenofibrate on type 1 diabetic retinopathy via inhibiting oxidative stress-mediated Wnt/β-catenin pathway activation. *Cell Tissue Res*. 2019;376(2):165–177. doi:10.1007/s00441-018-2974-z
27. Fu D, Yu JY, Connell AR, Hookham MB, McLeese RH, Lyons TJ. Effects of Modified Low-Density Lipoproteins and Fenofibrate on an Outer Blood-Retina Barrier Model: implications for Diabetic Retinopathy. *J Ocul Pharmacol Ther*. 2020;36(10):754–764. doi:10.1089/jop.2020.0068
28. Bedard K, Krause KH. The NOX family of ROS-generating NADPH oxidases: physiology and pathophysiology. *Physiol Rev*. 2007;87(1):245–313. doi:10.1152/physrev.00044.2005
29. Bandookwala M, Sengupta P. 3-Nitrotyrosine: a versatile oxidative stress biomarker for major neurodegenerative diseases. *Int J Neurosci*. 2020;130 (10):1047–1062. doi:10.1080/00207454.2020.1713776
30. Nakanishi A, Wada Y, Kitagishi Y, Matsuda S. Link between PI3K/AKT/PTEN Pathway and NOX Proteinin Diseases. *Aging Dis*. 2014;5 (3):203–211. doi:10.14336/AD.2014.0500203
31. Liu B, Deng X, Jiang Q, et al. Scoparone improves hepatic inflammation and autophagy in mice with nonalcoholic steatohepatitis by regulating the ROS/P38/Nrf2 axis and PI3K/AKT/mTOR pathway in macrophages. *Biomed Pharmacother*. 2020;125:109895. doi:10.1016/j.biopha.2020.109895
32. Moran E, Ding L, Wang Z, et al. Protective and antioxidant effects of PPARα in the ischemic retina. *Invest Ophthalmol Vis Sci*. 2014;55 (7):4568–4576. doi:10.1167/iovs.13-13127
33. Chen Q, Jiang N, Zhang Y, et al. Fenofibrate Inhibits Subretinal Fibrosis Through Suppressing TGF-β-Smad2/3 signaling and Wnt signaling in Neovascular Age-Related Macular Degeneration. *Front Pharmacol*. 2020;11:580884. doi:10.3389/fphar.2020.580884
34. Chen L, Liu P, Feng X, Ma C. Salidroside suppressing LPS -induced myocardial injury by inhibiting ROS -mediated PI 3K/Akt/ mTOR pathway in vitro and in vivo. *J Cell Mol Med*. 2017;21(12):3178–3189. doi:10.1111/jcmm.12871
35. Ma L, Li XP, Ji HS, Liu YF, Li EZ. Baicalein Protects Rats with Diabetic Cardiomyopathy Against Oxidative Stress and Inflammation Injury via Phosphatidylinositol 3-Kinase (PI3K)/AKT Pathway. *Med Sci Monit*. 2018;24:5368–5375. doi:10.12659/MSM.911455
36. Wang X, Yu C, Liu X, et al. Fenofibrate Ameliorated Systemic and Retinal Inflammation and Modulated Gut Microbiota in High-Fat Diet-Induced Mice. *Front Cell Infect Microbiol*. 2022;12:839592. doi:10.3389/fcimb.2022.839592
37. Beeharry N, Lowe JE, Hernandez AR, et al. Linoleic acid and antioxidants protect against DNA damage and apoptosis induced by palmitic acid. *Mutat Res*. 2003;530(1–2):27–33. doi:10.1016/S0027-5107(03)00134-9
38. Ahn JH, Kim MH, Kwon HJ, Choi SY, Kwon HY. Protective Effects of Oleic Acid Against Palmitic Acid-Induced Apoptosis in Pancreatic AR42J Cells and Its Mechanisms. *Korean j Phys Pharmacol*. 2013;17(1):43–50. doi:10.4196/kjpp.2013.17.1.43
39. Yoon YH, Cho KS, Hwang JJ, Lee SJ, Choi JA, Koh JY. Induction of lysosomal dilatation, arrested autophagy, and cell death by chloroquine in cultured ARPE-19 cells. *Invest Ophthalmol Vis Sci*. 2010;51(11):6030–6037. doi:10.1167/iovs.10-5278
40. Datta S, Cano M, Ebrahimi K, Wang L, Handa JT. The impact of oxidative stress and inflammation on RPE degeneration in non-neovascular AMD. *Prog Retin Eye Res*. 2017;60:201–218. doi:10.1016/j.preteyeres.2017.03.002
41. Chen J, Li L, Zhou Y, Zhang J, Chen L. Gambogic acid ameliorates high glucose- and palmitic acid-induced inflammatory response in ARPE-19 cells via activating Nrf2 signaling pathway: ex vivo. *Cell Stress Chaperones*. 2021;26(2):367–375. doi:10.1007/s12192-020-01182-1
42. Roddy GW, Rosa RH, Viker KB, et al. Diet Mimicking "Fast Food" Causes Structural Changes to the Retina Relevant to Age-Related Macular Degeneration. *Curr Eye Res*. 2020;45(6):726–732. doi:10.1080/02713683.2019.1694156
43. Keeling E, Lynn SA, Koh YM, et al. A High Fat "Western-style" Diet Induces AMD-Like Features in Wildtype Mice. *Mol Nutr Food Res*. 2022;66: e2100823.
44. Asare-Bediako B, Noothi SK, Li Calzi S, et al. Characterizing the Retinal Phenotype in the High-Fat Diet and Western Diet Mouse Models of Prediabetes. *Cells*. 2020;9(2):464. doi:10.3390/cells9020464
45. Chen Y, Hu Y, Lin M, et al. Therapeutic effects of PPARα agonists on diabetic retinopathy in type 1 diabetes models. *Diabetes*. 2013;62 (1):261–272. doi:10.2337/db11-0413
46. Kim J, Ahn JH, Kim JH, et al. Fenofibrate regulates retinal endothelial cell survival through the AMPK signal transduction pathway. *Exp Eye Res*. 2007;84(5):886–893. doi:10.1016/j.exer.2007.01.009
47. Grygiel-Górniak B. Peroxisome proliferator-activated receptors and their ligands: nutritional and clinical implications--a review. *Nutr J*. 2014;13 (1):17. doi:10.1186/1475-2891-13-17
48. Yu J, Liu S, Chen L, Wu B. Combined effects of arsenic and palmitic acid on oxidative stress and lipid metabolism disorder in human hepatoma HepG2 cells. *Sci Total Environ*. 2021;769:144849. doi:10.1016/j.scitotenv.2020.144849
49. Huang X, Liu G, Guo J, Su Z. The PI3K/AKT pathway in obesity and type 2 diabetes. *Int J Biol Sci*. 2018;14(11):1483–1496. doi:10.7150/ijbs.27173
50. Huang F, Chen J, Wang J, Zhu P, Lin W. Palmitic Acid Induces MicroRNA-221 Expression to Decrease Glucose Uptake in HepG2 Cells via the PI3K/AKT/GLUT4 Pathway. *Biomed Res Int*. 2019;2019:8171989. doi:10.1155/2019/8171989
51. Zha X, Wu G, Zhao X, et al. PRDX6 Protects ARPE-19 Cells from Oxidative Damage via PI3K/AKT Signaling. *Cell Physiol Biochem*. 2015;36 (6):2217–2228. doi:10.1159/000430186

52. Song M, Du Z, Lu G, Li P, Wang L. Syringic acid protects retinal ganglion cells against H2O2-induced apoptosis through the activation of PI3K/Akt signaling pathway. *Cell Mol Biol*. 2016;62(6):50–54.
53. Qiu F, Tong H, Wang Y, Tao J, Wang H, Chen L. Recombinant human maspin inhibits high glucose-induced oxidative stress and angiogenesis of human retinal microvascular endothelial cells via PI3K/AKT pathway. *Mol Cell Biochem*. 2018;446(1–2):127–136. doi:10.1007/s11010-018-3280-5